RSC Advances

PAPER

View Article Online
View Journal | View Issue

Cite this: *RSC Adv.*, 2019, **9**, 18406

Preparation of ZnO nanoparticle loaded amidoximated wool fibers as a promising antibiofouling adsorbent for uranium(VI) recovery†

Haichuan Ma,[a] Fan Zhang,[b] Qiaoyu Li,[a] Guobing Chen,[a] Sheng Hu[b] and Haiming Cheng *[ac]

Received 20th May 2019
Accepted 6th June 2019

DOI: 10.1039/c9ra03777b

rsc.li/rsc-advances

In this study, nano-ZnO loaded amidoxime-functionalized wool fibers (wool-AO@ZnO) were synthesized by radiation-induced copolymerization and *in situ* co-precipitation as a novel adsorbent with good antibiofouling properties for uranium recovery. The prepared adsorbent was characterized by SEM-EDS and FT-IR spectroscopy. Batch adsorption experiments showed that the prepared wool-AO@ZnO have a good uranium adsorption property at pH 6.0–9.0. Meanwhile, wool-AO@ZnO displayed a good inhibition of aerobic bacteria such as *S. aureus* and *E. coli*; of anaerobic bacteria; of sulfate reducing bacteria; of fungus *C. albicans* and of mildew *Aspergillus niger*. After four cyclic cultivations with microorganisms, the inhibition rate of wool-AO@ZnO to *E. coli* and *S. aureus* still remains at 77.8% and 84.9%, respectively; and a good adsorption capacity for uranium(VI) was maintained. The prepared wool-AO@ZnO could be a promising antibiofouling adsorbent for the recovery of uranium(VI) from seawater.

1. Introduction

Nuclear energy plays an important role in the energy industry. Uranium is the most essential resource for nuclear power. Extraction of uranium from seawater has been paid more and more attention in many countries since the terrestrial uranium supply is limited. Although the uranium concentration in seawater is only approximately 3 ppb, the total amount of uranium in seawater is over 4.5 billion tons, which is around 1000 times larger than the entire proven uranium reserves on land.[1]

Several approaches have been developed for uranium extraction including solvent extraction,[2] flotation,[3] ion exchange,[4] biological collection,[5] precipitation[6] and adsorption.[7] In comparison with other methods, the adsorption technique has been thought of as a promising method due to its ease of operation, advantageous uranium enrichment, and low cost. However, since the complication of the ocean climate and the presence of large excess competing ions in seawater, it is clear that the key roles of the adsorbents in uranium extraction from seawater are their selectivity to uranium ions, extraction efficiency, and its physical stability in the ocean environment. Amidoxime groups based adsorbents have been reported showing good selectivity toward uranium, therefore, various matrixes have been functionalized with amidoxime groups for uranium adsorption including polymeric fibers, hydrogels, metal organic frameworks, and natural biopolymers.[8–10] Amidoxime functionalized wool fibers have been developed for recovery of uranium due to its good hydrophilicity and good physical stability.[10–13]

Recently, the problem of biofouling in decreasing adsorption performance and the corrosion of adsorbent has been noted by Park *et al.*[14] and Hu *et al.*[15] Due to the concentration of uranium in seawater is critical low, the adsorbents were immersed in the seawater usually for several weeks. Therefore, a variety of microorganisms such as aerobic bacteria, anaerobic bacteria and fungus will adhere on the surface of the adsorbents and thus the biofouled surface might occur. Biofouling can decrease the adsorbents stabilities, adsorption efficiency, and elution efficiency. It was noted that the key reason of biofouling is the rapidly binding of the microorganisms on the adsorbent matrix in the ocean environment. Therefore, the development of good antimicrobial adsorbents should be a potential strategy to prevent the biofouling. For instance, Zhang *et al.*[16] prepared a polymeric nonwoven fabric co-functionalized with guanidine and amidoxime, and found that the introduced guanidine groups could inhibit the growth of *Escherichia coli* (*E. coli*) on the adsorbent surface. Quaternary ammonium derivatives, guanidine derivatives, and inorganic nanoparticles have been employed on wool fibers for obtaining antibacterial functions.[16–18] In the other hand, inorganic nanoparticles such as Ag,

[a]*The Key Laboratory of Leather Chemistry and Engineering of Ministry of Education, Sichuan University, Chengdu 610065, China*

[b]*Institute of Nuclear Physics and Chemistry, China Academy of Engineering Physics, Mianyang 621900, Sichuan, China*

[c]*National Engineering Laboratory for Clean Technology of Leather Manufacture, Sichuan University, Chengdu 610065, Sichuan, China. E-mail: chenghaiming@scu.edu.cn*

† Electronic supplementary information (ESI) available: Adsorption isotherms and adsorption kinetics fitting data. See DOI: 10.1039/c9ra03777b

ZnO, and TiO_2 showed a widely range of antibacterial activity. ZnO have shown excellent antibacterial effect on fabric films and polymer fibers.[19–21] In our previous work,[11] nano TiO_2 loaded amidoximated wool fibers could inhibit the growth of *E. coli* and *Staphylococcus aureus* (*S. aureus*); and maintain good uranium adsorption capacity. The two investigated bacteria are belonging to aerobic bacteria. However, besides aerobic bacteria, anaerobic bacteria and fungi are also found in the ocean. Therefore, the biofouling resistance properties of the promising uranium extraction adsorbents should be evaluated for inhibiting microorganisms, including aerobic bacteria, anaerobic bacteria, and fungi.

Herein, a novel adsorbent wool-AO@ZnO was prepared by loading ZnO nanoparticles on amidoxime functionalized wool fibers by *in situ* co-precipitation and radiation-induced graft copolymerization. ZnO nanoparticles were used for the enhancement of antibacterial properties to amidoxime-functionalized wool fibers. The uranium adsorption property and antibacterial characteristics such as inhibiting of aerobic bacteria (Gram-negative and Gram-positive), anaerobic bacteria, and fungi were evaluated.

2. Experimental

2.1. Reagents and materials

Merino wool fibers were purchased from Qige Textile Company (Tongxiang, China). Acrylonitrile and methacrylate were purchased from Kelong Chemicals (Chengdu, China). Zinc oxide (ZnO) (size 30 ± 10 nm) was purchased from Aladdin (Shanghai China). The stock solution of uranium (1000 mg L^{-1}) was prepared by dissolving $UO_2(NO_3)_2 \cdot 6H_2O$ in deionized water. Uranium(VI) standard solution at 1000 ppm concentration was supplied by National Analysis and Testing Center (Beijing China). All other regents were analytical grade and used without further purification.

2.2. Preparation of wool-AO@ZnO[10–12]

Pristine wool fibers were degreased by acetone. After degreasing, the wool fibers were immersed into 1000 mL of 1% NaOH (m/v) and treated at 50 °C for 10 min to open the cuticle of the wool fibers, which were then taken out and washed with deionized water till the pH value of the solution was at neutral. Then the wool fibers were dried to constant weight at 40 °C.

Co-irradiation grafting method was used for preparation of nano-ZnO particles loaded amidoxime functionalized wool fibers (wool-AO@ZnO). Briefly, 1.0 g of the pretreated wool fibers were mixed with 7 mL of acrylonitrile, 3 mL of methacrylic acid, and 3 mL of deionized water, and a certain amount of ZnO nanoparticles (5–20 mg) in a weighing bottle, which then was sealed with an aluminum foil. The sealed bottle was then radiated with 200 kGy irradiation dose under electron beam (dose rate 15 kGy m^{-1}, beam current 12 kW). Afterwards, the wool fibers were taken out and washed with acetone and deionized water three times, respectively; to remove homopolymers (polyacrylonitrile) and un-reacted monomers. The product finally dried at 40 °C to constant weight that designated as wool-AN@ZnO.

To obtain amidoxime groups, 1.0 g of wool-AN@ZnO was placed into 50 mL of neutralized $NH_2OH \cdot HCl$ methanol solution (methanol: water = 1 : 1, pH 7.0). The mixture was refluxed at 70 °C for 5 h, after which the wool fibers was washed with methanol thoroughly and dried at 40 °C. The obtained adsorbent was designated as wool-AO@ZnO. As controls, wool-AN and wool-AO fibers without adding ZnO nanoparticles were prepared following the same procedures as described above.

2.3. Characterization

The FT-IR spectra of pristine wool fibers, wool-AN@ZnO and wool-AO@ZnO were recorded on a Nicolet iS10 FT-IR spectrophotometer (Thermo Scientific, USA) by the KBr pellet method in a range from 4000 to 600 cm^{-1}. The morphologies of the fibers were observed by a JSM-F7500 Scanning electron microscope (SEM) (Japan Electron Optical Laboratory Co., LTD, Japan). The elemental compositions of the samples were measured by a 51-XMX0019 X-Max Energy-dispersive X-ray spectroscopy (EDXS) (Oxford Instruments, UK). The nitrogen adsorption isotherms of the samples were detected by a Tristar 3000 surface area and porosity analyzer (Micromeritics, USA) at 77 K. The surface area of samples was calculated by Barrett–Emmett–Teller (BET) equation. All tests were run in triplicate.

2.4. Batch adsorption experiments

Batch experiment was applied for studying uranium(VI) adsorption by wool-AO@ZnO. Briefly, 10.0 mg of wool-AO@ZnO absorbent and 20 mL of a set concentration of uranium(VI) solution were placed in a 50 mL plastic flask, shaking at a WS-300R thermostat shaker (Wiggens, Germany) with 100 rpm for 24 h at 25 °C. While studying the effect of initial pH on the adsorption, the pH value of the solution varied from 3.0 to 9.0, which was adjusted by 0.1 M NaOH and 0.1 M HCl. All adsorption experiments were conducted with an initial uranium(VI) concentration of 50 ppm for 24 h at 25 °C. The kinetic studies were performed at pH 8.0 with temperature varying from 20–40 °C. The isotherm studies were performed with the initial uranium(VI) concentrations varying from 10–500 ppm. The concentration of uranium(VI) before and after adsorption was determined by a 2300 DV inductively coupled plasma atomic emission spectrometry (ICP-AES) (PerkinElmer, USA).The amount of the adsorption to uranium (mg g^{-1}) was calculated by eqn (1):

$$q_e = \frac{C_0 - C_e}{m} \times v \quad (1)$$

where q_e (mg g^{-1}) is the equilibrium adsorption capacity of uranium; C_0 (mg L^{-1}) is the initial concentration and C_e (mg L^{-1}) is the concentration at equilibrium states of adsorption; m and v represent the quality of absorbent (g) and volume of uranium solution (L), respectively.

2.5. Antibacterial evaluation

2.5.1. Aerobic bacteria and fungus *Candida albicans*. In this study, three aerobic bacteria species, Gram-negative *E. coli*, Gram-positive *S. aureus*, and fungus *Candida albicans* (*C. albicans*) were selected to evaluate the antimicrobial properties of wool-AO@ZnO against aerobic bacteria. The evaluation tests were based on Chinese Standard GB/T 20944.3-2008 (Textiles – evaluation of antibacterial activity: shake flask method) with a slight modification. Briefly, liquid lysogeny broth (LB) medium was used for culture of *E. coli* and *S. aureus*, while *C. albicans* was cultured in Sabouraud medium (SAB) (glucose 40 g L^{-1}, peptone 10 g L^{-1}). Firstly, bacteria were cultivated in their medium at 35 °C for 18 h then the cell suspensions were diluted with PBS (0.03 mol L^{-1}, pH 7.2–7.4) to cell density (counted in colony-forming units (CFU)) between 1–3 × 10^7 CFU mL^{-1}. 750 mg of wool-AO@ZnO, 49 mL of PBS, and 1 mL of cell suspensions was put into a 150 mL flask, keeping cell concentration at 2–6 × 10^5 CFU mL^{-1}. Then the flask was shaken on a thermostat shaker at 35 °C for 18 h exposed under visible light. Subsequently, 1.0 mL of cell suspensions was taken out for preparing a series of tenfold dilution with PBS, plated out in LB agar. The plates were incubated at 35 °C for 18 h (for *C. albicans*, at 28 °C for 48 h) and then counted their colony-forming units. Pristine wool fibers were used as a control. The reduction of CFU (R) was calculated by the eqn (2):

$$R\% = \frac{(A - B)}{A} \times 100\% \quad (2)$$

where A is average number of bacterial colonies in pristine wool, and B is average number of bacterial colonies on wool-AO@ZnO.

To investigate the antibacterial activity of wool-AO@ZnO under prolonged bacterial environment, 15 mg of wool-AO@ZnO was applied to follow the experiments of successive uranium(VI) adsorption.

2.5.2. Anaerobic bacteria. Sulfate reducing bacteria (SRB) were used for the evaluation of the inhibition of wool-AO@ZnO to anaerobic bacteria. Firstly, 140 mL of liquid medium (pH was adjusted at 6.85) was sterilized at 120 °C for 20 min (yeast extract 1 g L^{-1}, $K_2HPO_4 \cdot 3H_2O$ 0.5 g L^{-1}, Na_2SO_4 0.5 g L^{-1}, $CaCl_2 \cdot H_2O$ 0.1 g L^{-1}, NH_4Cl 1.0 g L^{-1}, $MgSO_4 \cdot 7H_2O$ 2.0 g L^{-1}, sodium lactate (70%) 3.5 g L^{-1}, $(NH_4)_2Fe(SO_4)_2 \cdot 6H_2O$ 0.5 g L^{-1}, and ascorbic acid 0.1 g L^{-1}). In particular, $MgSO_4 \cdot 7H_2O$, $(NH_4)_2Fe(SO_4)_2 \cdot 6H_2O$ and ascorbic acid were sterilized for 30 min by UV lamp. Secondly, 10 mL of SRB solution was added to the prepared liquid medium and cultivated at 33.5 °C for 3 days to enrichment of SRB strains. To obtain purified strains, this process was repeated 3 times. Thirdly, 10 mL of medium containing purified SRB strains was mixed with 140 mL of liquid medium for a few days till some black precipitate could be observed at the bottom of the flask. Then, 5 mL of medium containing SRB strains was taken out and mixed with 0.1 g of wool-AO@ZnO in a test tube, which was incubated at 35 °C for 2 h, then 1 mL of solution was taken out to prepare a series of tenfold dilution with liquid medium (pH 7.0). The concentration of SRB strains was counted according to MPN method.[22] Pristine wool fibers were used as a control.

2.5.3. Mildew. *Aspergillus niger* was selected in this study for investigating the inhibition properties of wool-AO@ZnO to mildew. To prepare liquid potato medium, 200 g of potatoes was cut into small pieces (1.0 cm^3) and then was boiled for 20–30 min. After filtration, the liquid was calibrated to 1000 mL. 50 mL of the liquid potato medium was used for enrichment of *Aspergillus niger* for 10 h at 37 °C. After enrichment, the bacterial solution was diluted 5 times with liquid potato medium (number of spores ~10^4). 200 μL of the diluted solution containing *Aspergillus niger* was taken out and absorbed by wool-AO@ZnO. It was incubated at 37 °C and 85% humidity for 5 days. The growth of the mildew on the samples was observed periodically.

3. Results and discussion

3.1. Characteristics of wool-AO@ZnO

The FT-IR spectra of pristine wool, wool-AN@ZnO and wool-AO@ZnO were shown in Fig. 1. The peak around 3300 cm^{-1} belongs to –OH and $–NH_2$ groups of wool matrix. The peaks at 1632.8, 1545.7, and 1387.7 cm^{-1} are assigned to stretching vibration of –C=O (amide I), bending vibration of –N–H (amide II), and stretching vibration of C–N (amide III), respectively.[13] The FT-IR profile of wool-AN@ZnO showed a new peak at 2245.5 cm^{-1} which ascribes to stretching vibration of –C≡N. Meanwhile, the stretching vibration peak (1734.8 cm^{-1}) attributed to C=O, and the broad strong peak at 932.9 cm^{-1} belongs to the bending vibration of –OH of carboxylic acid, indicating that acrylonitrile and methacrylic acid was successfully grafted onto wool fibers. After amidoximation, the disappearance of the peak at 2245.5 cm^{-1} and a new observed peak at 929.9 cm^{-1} belongs to the stretching of N–O band of amidoxime group.[10] The results suggested that the amidoximation reaction was success.

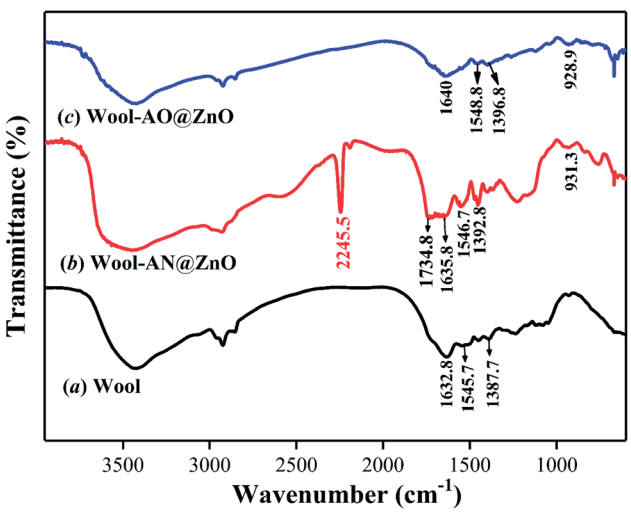

Fig. 1 FT-IR spectra. (a) Pristine wool, (b) wool-*g*-AN-@ZnO and (c) wool-*g*-AO-@ZnO.

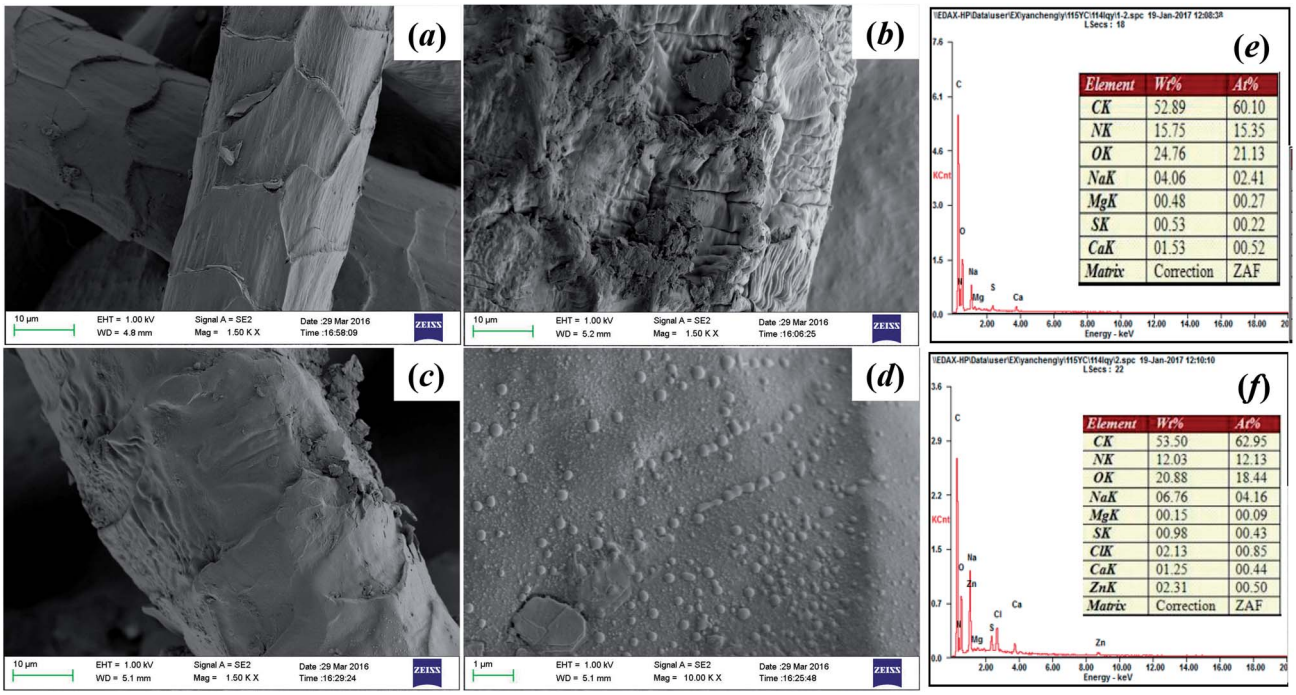

Fig. 2 The SEM and EDS profiles of wool samples. (a) Pristine wool; (b) wool-AO; (c and d) wool-AO@ZnO; (e) EDS profiles of wool-AO; (f) EDS profiles of wool-AO@ZnO.

SEM and EDS profiles of pristine wool and wool-AO@ZnO were shown in Fig. 2. A clear and smooth scale layer could be observed on the SEM profiles of pristine wool (Fig. 2a), illustrating that the structure of wool was relatively complete before co-irradiation reaction. While after co-irradiation the exterior structure of wool-AO was damaged seriously (Fig. 2b) and the surface of wool-AO became rough since the polymers were grafted on. Moreover, the introduction of ZnO nanoparticles imparted the surface of wool fibers uniformly covered with a size of 20–40 nm nanoparticles (Fig. 2d). The EDS profiles of wool-AO and wool-AO@ZnO characterized the elemental composition on the fiber surface. In comparison with wool-AO, element Zn was observed on the surface of wool-AO@ZnO (Fig. 2f), which further confirming that the ZnO nanoparticles were successfully loaded onto the wool fibers.

3.2. Uranium(VI) adsorption experiments

3.2.1. Effect of the initial pH. Uranium(VI) adsorption by wool-AO@ZnO was studied in 50 mL tubes containing 20 mL of 50 mg L^{-1} uranium(VI) solution with 10 mg of adsorbent at 25 °C for 10 h by varying the initial pH of the solution from 3.0 to 9.0 (Fig. 3a). It can be seen that the uranium adsorption capacity increases from 25.92 to 72.53 mg g^{-1} with the increase in pH from 3.0 to 9.0. When the initial pH was at 3.0, the adsorption capacity of wool-AO@ZnO was 25.92 mg g^{-1}. Meanwhile, amidoxime groups on wool-AO@ZnO are protonated, which repels uranium(VI) cationic species, while under this pH environment, uranium(VI) predominant exists in UO_2^{2+}, therefore, the adsorption capacity is relatively low. With pH increasing from 3.0 to 6.0, UO_2^{2+} hydrolyzes as less positively forms or even negative forms as $UO_2(OH)^+$ and $UO_2NO_3^+$, $UO_2(CO_3)$, $UO_2(CO_3)_2^{2-}$, and $UO_2(CO_3)_3$.[4–24] On the other hand, amidoxime groups (pH_{ZCP} 4.3)[25] would be gradually deprotonated; and the surface charge on wool-AO@ZnO would be changed from positive to negative, leading the increase of uranium adsorption. It is interesting to see that when the pH is higher than 6.0, the adsorption capacity keep increase gradually, which may due to ZnO nanoparticles have a higher pH_{ZCP} (9.3)[26] than amidoxime groups, leading the adsorption capacity enhanced and stable at pH 6.0–9.0.

3.2.2. Effect of dosage of ZnO. The effect of the dosage of ZnO on wool-AO@ZnO to adsorption was carried out in 50 mL tubes containing 20 mL of 50 mg L^{-1} uranium(VI) solution at pH 8.0 with 10 mg of adsorbent at 25 °C for 10 h (Fig. 3b). It revealed that the uranium(VI) adsorption capacity shows a rising tendency with increasing the dosage of ZnO, which had a peak of uranium(VI) adsorption at 62.8 mg g^{-1} when the dosage of ZnO was up to 1.0%. The results can be explained in two aspects. ZnO nanoparticles loaded onto the surface of wool-AO@ZnO display a positive charge (pH_{ZCP} 9.3), while uranium(VI) is mainly in the form of negatively charged when pH at 8.0, which contributed to the adsorption of uranium on wool-AO@ZnO. On the other hand, nano-ZnO itself showed adsorption property to uranyl groups.[27–29] Nevertheless, excessive dosage of ZnO can weaken the surface effect of ZnO nanoparticles for generation of agglomerated particles which reduces the adsorption sites,[30] which drop down the adsorption capacity.

3.2.3. The effect of contact time. The effect of contact time on the adsorption of uranium(VI) onto wool-AO@ZnO was

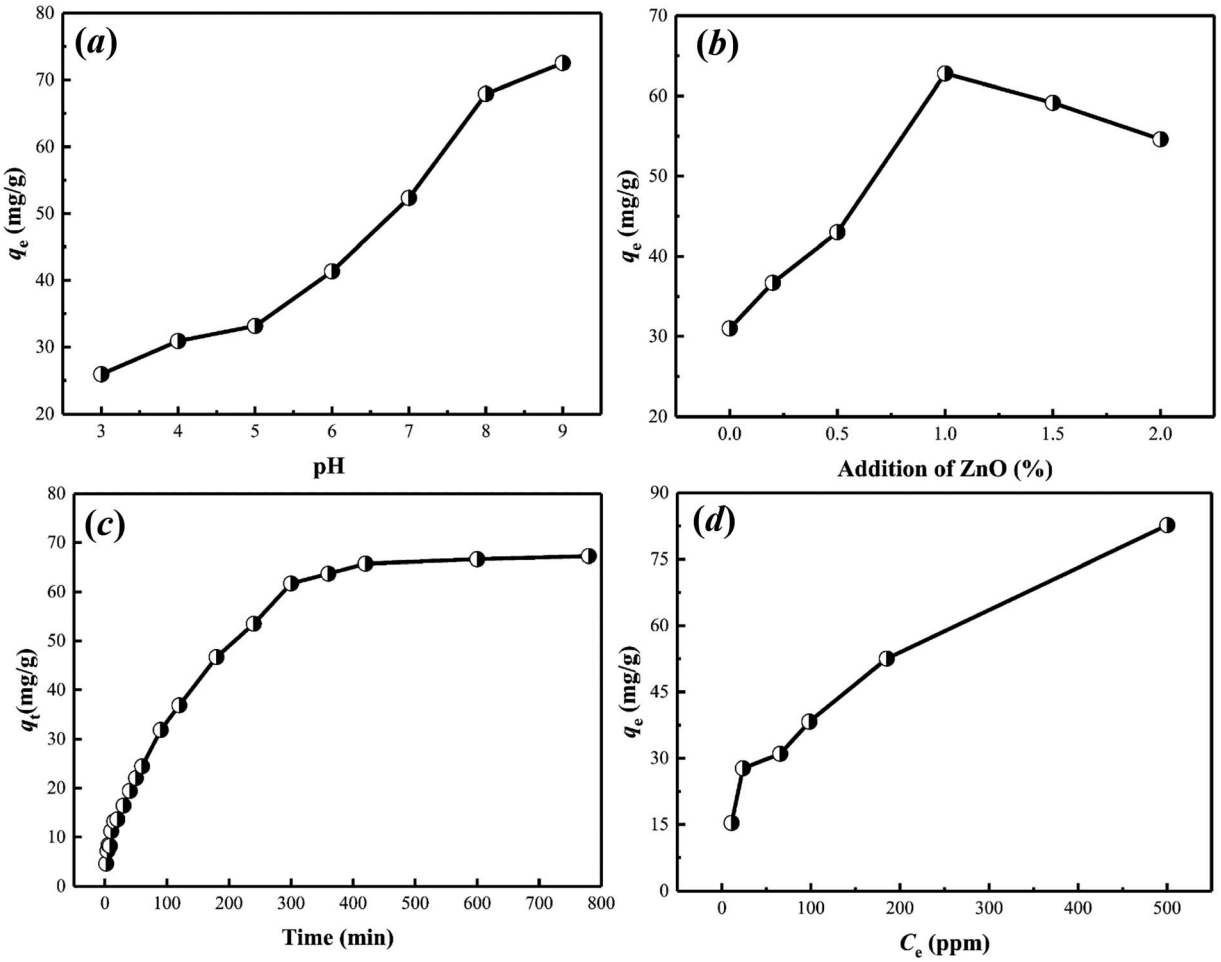

Fig. 3 Uranium adsorption by wool-AO@ZnO. (a) Initial pH, (b) dosage of ZnO, (c) contact time, (d) initial concentration of uranium.

studied in 250 mL Erlenmeyer flasks containing 100 mL of 50 mg L^{-1} uranium(VI) solution with 10 mg of wool-AO@ZnO at 25 °C and pH 8.0. The relationship between adsorption amount (q_t) and contact time (t) is shown in Fig. 3c. It is clear to show that the rate of adsorption uranium(VI) onto wool-AO@ZnO was rapid during the first 100 min, and then slowed down gradually to reach the equilibrium at around 400 min. The adsorption capacity at equilibrium is 62.52 mg g^{-1}. The rapid adsorption rate might due to enough active sites available for adsorption at the early adsorption stage. The saturation of active adsorption sites and the decrease in uranium(VI) concentration cause the adsorption rate slow down. To ensure the adsorption process reaches equilibrium, the subsequent experiments were performed with 10 h.

Kinetic models like pseudo-first-order, pseudo-second-order, and Elovich models[31] were applied for fitting the experimental data (Fig. S1†). The calculated parameters are listed in Table 1. The results indicate that the kinetic behavior of uranium(VI) adsorption on wool-AO@ZnO is fitted well with pseudo-second-order model, with the correlation coefficient (R^2) value of 0.99. The result implies that chemical adsorption was responsible for the adsorption of uranium(VI) by wool-AO@ZnO, which is similar to our previous report.[11]

Table 2 Parameters of Langmuir and Freundlich models for uranium adsorption by wool-AO@ZnO

Langmuir			Freundlich		
k_L (L g^{-1})	q_m (mg g^{-1})	R^2	k_F	n	R^2
0.0095	95.6022	0.9286	6.2864	2.5560	0.8796

Table 1 Kinetic parameters for uranium adsorption by wool-AO@ZnO

Pseudo-first order			Pseudo-second order			Elovich		
k_1	q_e	R^2	k_2	q_e	R^2	α	β	R^2
12.9482	31.0270	0.8952	0.0002	75.5858	0.9964	3.0538	0.0802	0.9208

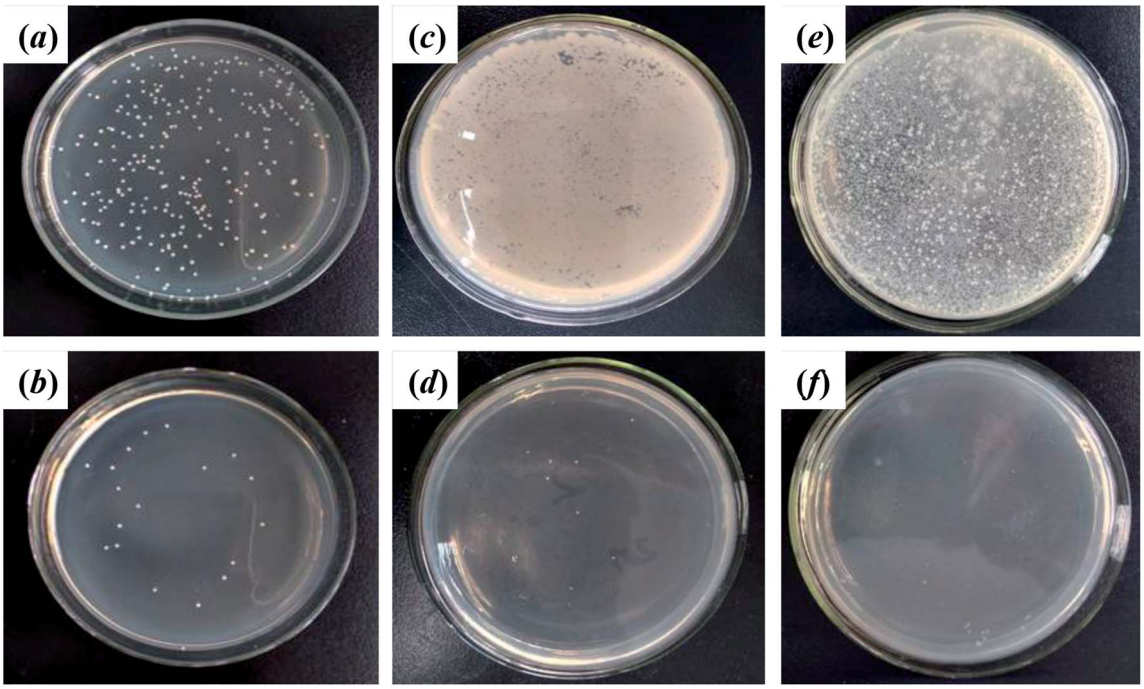

Fig. 4 Antibacterial properties of wool fiber. (a) Wool-AO-@ZnO and (b) pristine wool cultured with *E. coli*; (c) wool-AO-@ZnO and (d) pristine wool cultured with *S. aureus*; (e) wool-AO-@ZnO and (f) pristine wool cultured with *C. albicans*.

3.2.4. Effect of initial concentration of uranium(VI) ions. The effect of the initial concentration of uranium(VI) on the adsorption was carried out at 25 °C using various initial concentrations (10–500 mg L^{-1}) at pH 4.0, since while the pH is above 4.0, precipitation may be occurred at a high uranium(VI) concentration. The results showed that the adsorption capacity increases with increasing the initial concentration of uranium(VI) (Fig. 3d). In order to elucidate the nature of the adsorption process and adsorption mechanism, the experimental data were evaluated with adsorption isotherm models, Langmuir model[32] and Freundlich model[33] (Fig. S2,† Table 2). The results show that the Langmuir model is applicable to fit the behavior of uranium(VI) adsorption onto wool-AO@ZnO, with an R^2 value of 0.93, suggesting a monolayer uniform adsorption mode for wool-AO@ZnO adsorbing uranium(VI). The maximum uranium(VI) adsorption capacity (qm) of wool-AO@ZnO calculated by the Langmuir isotherm function was 95.60 mg g^{-1}.

3.3. Antimicrobial evaluation

3.3.1. Aerobic bacteria. In this study, the properties of wool-AO@ZnO against aerobic bacteria *E. coli* and *S. aureus*

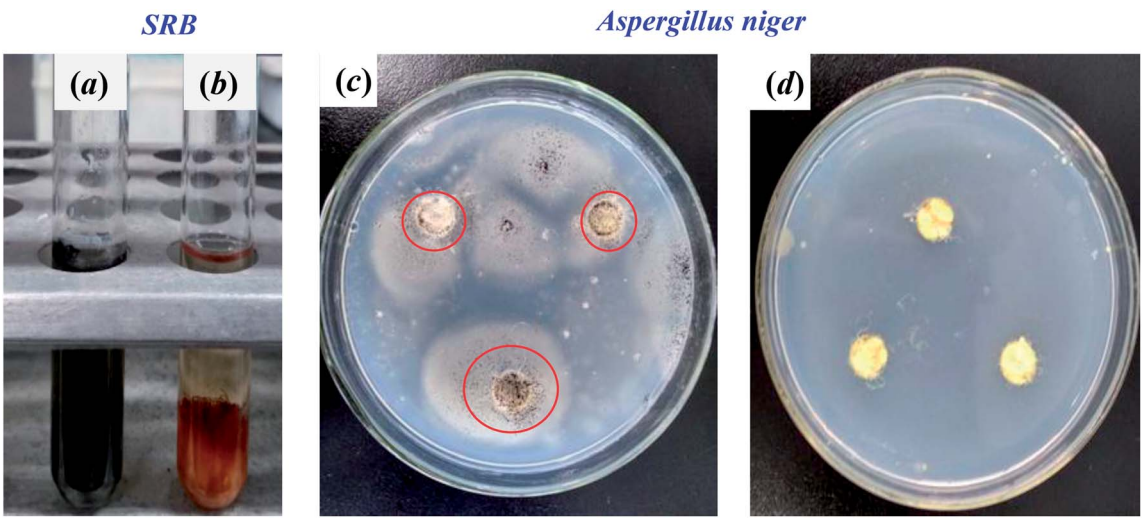

Fig. 5 Antibacterial properties of wool fibers. (a) Wool-AO-@ZnO and (b) pristine wool cultured with SRB; (c) wool-AO-@ZnO and (d) pristine wool cultured with *Aspergillus niger*.

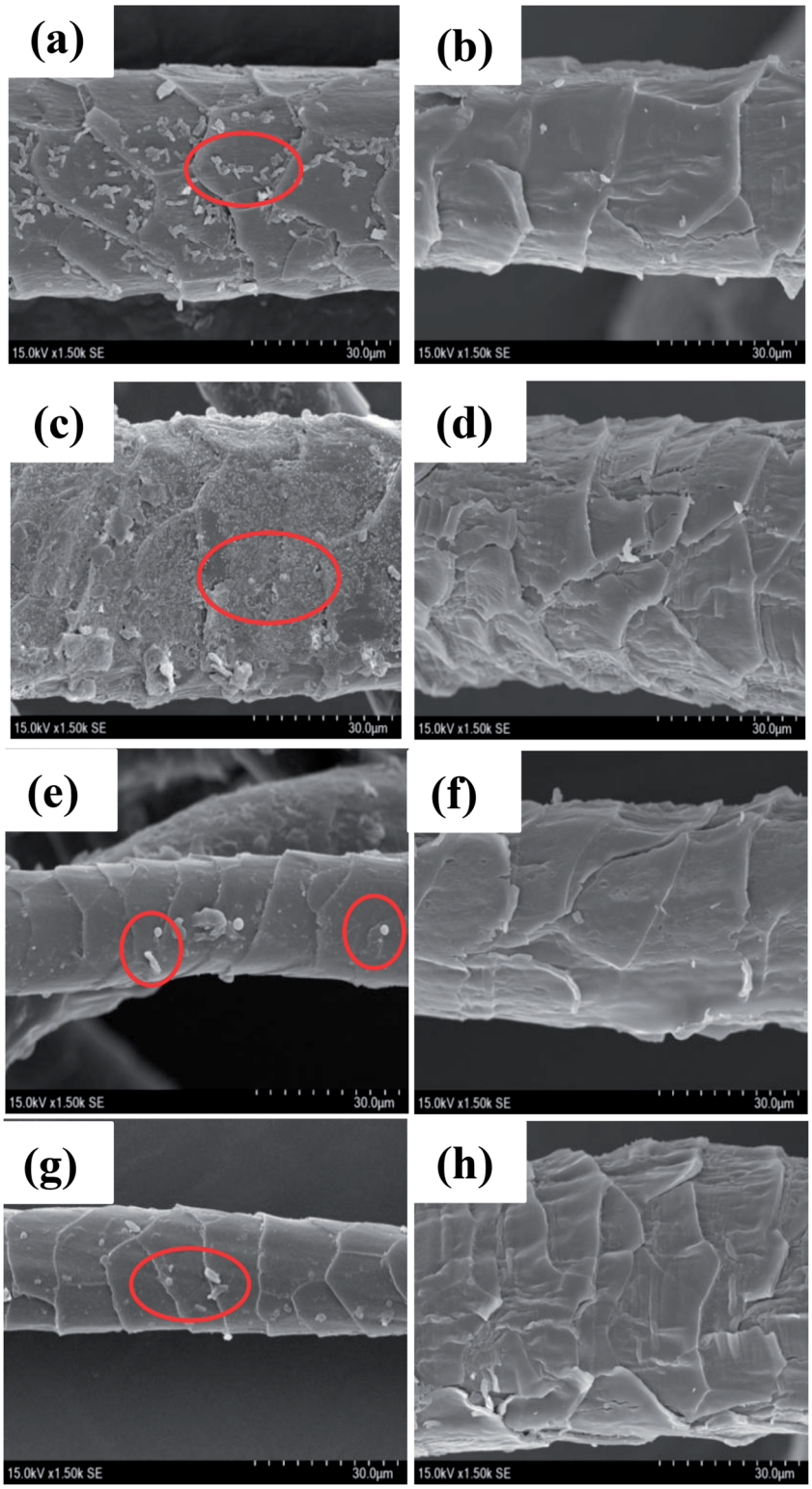

Fig. 6 SEM images of wools cultured with *E. coli* (a), *S. aureus* (c), *C. albicans* (e), SRB (g) and SEM images of wool-AO@ZnO cultured with *E. coli* (b), *S. aureus* (d), *C. albicans* (f), SRB (h) for 24 h.

were investigated by culturing them together in LB medium at 35 °C for 18 h; and then taking 1 mL of the medium cultured on LB agar plate. The pristine wool fibers showed no inhibition effect to both Gram-negative and Gram-positive bacteria, many colonies of survival bacteria were found on the plate (Fig. 4a and c). Moreover, the living bacteria were occupied among the whole culture medium after 18 h cultivation. In contrast, culturing with wool-AO@ZnO, only a few of bacteria could be observed

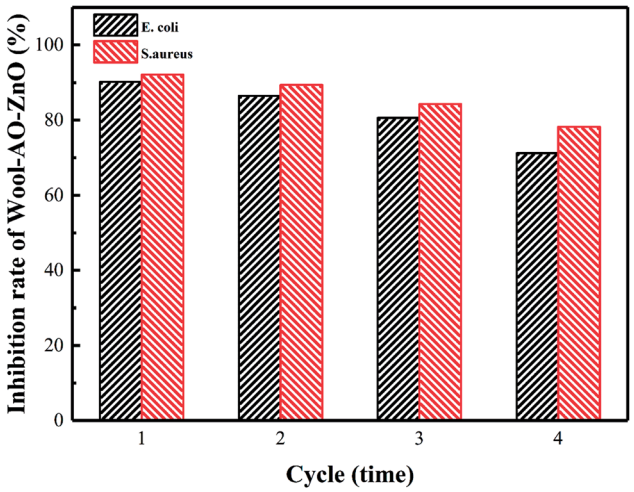

Fig. 7 Antibacterial properties of wool-AO@ZnO after cyclic cultivation and uranium adsorption and desorption.

Table 3 Uranium adsorption after contacting with bacteria 4 cycles

Sample	*E. coli* (mg g^{-1})	*S. aureus* (mg g^{-1})
Wool-AO	17.7	15
Wool-AO-@ZnO	46.5	57.6

(Fig. 4b and d). The results illustrate that wool-AO@ZnO was possessed of excellent antibacterial effect to aerobic bacteria. The results indicate good antimicrobial properties of wool-AO@ZnO should be due to the loaded ZnO nanoparticles. Two mechanisms are related to ZnO nanoparticles restrain the growth of microorganisms. ZnO nanoparticles under light will produce highly active free radicals such as hydroxyl radicals ($OH^{\bullet}$), superoxide anion radicals ($O_2^{\bullet-}$) and perhydroxyl radicals ($HO_2^{\bullet}$) which damage the cell structure of microorganisms, leading to the destruction and complete decomposition.[34] Moreover, ZnO nanoparticles will release Zn^{2+} ions that may bind together with protein and enzyme as well as microbial nucleic acids to prevent microbial replication.[35] Furthermore, the reduction of CFU showed that the antibacterial efficiency of wool-AO@ZnO against *S. aureus* and *E. coli* was both at 99.9%.

3.3.2. Anaerobic bacteria (sulfate reducing bacteria). Sulfate reducing bacteria (SRB) are a kind of anaerobic microorganism utilizing reduction of sulfate to provide energy. When SRB largely proliferate, sulfate (SO_4^{2-}) is converted into S^{2-}. Meanwhile, Fe^{2+} can combine with S^{2-} in aqueous solution, forming FeS, a black precipitation. Moreover, wool-AO@ZnO showed a good restraining effect on SRB (Fig. 5). No precipitations could be observed in the tubes containing wool-AO@ZnO (Fig. 5a), while black precipitations could be observed in the tubes containing pristine wool fibers, illustrating pristine wool fibers showed no inhibition to the growth of SRB (Fig. 5b). Quantitative evaluation showed that the antibacterial efficiency of wool-AO@ZnO to SRB was at 95%, which suggesting that wool-AO@ZnO can effectively inhibit the growth of anaerobic bacteria.

3.3.3. Fungus *C. albicans*. The properties of wool-AO@ZnO against fungus *C. albicans* were investigated by culturing in SAB medium at 35 °C for 18 h; and then taking 1.0 mL of the medium cultured on LB agar plate. It can be seen that only several of *C. albicans* colony was existed in the medium with wool-AO@ZnO (Fig. 4c); while many colonies could be observed in the medium cultured with the pristine wool fibers (Fig. 4f). The result indicates that wool-AO@ZnO can inhibit the growth of fungi. The reduction of CFU calculation showed that the inhibition of wool-AO@ZnO to fungi was 92.6% against *C. albicans*. The differences in antibacterial and antifungal activity might due to the structure of fungi was less sensitive to ZnO nanoparticles than bacteria.[36]

3.3.4. Mildew *Aspergillus niger*. The inhibition of wool-AO@ZnO to mildew *Aspergillus niger* was also investigated. The liquid medium was fully absorbed by wool-AO@ZnO, meanwhile, *Aspergillus niger* was also attached to samples. Reproduction of *Aspergillus niger* mainly depends on spore proliferation differing from other fungi. It is clearly to see that there were many black spores around the pristine wool fibers (Fig. 5c), moreover, black spores of *Aspergillus niger* were scattered onto other region of the plate. In contrast, wool-AO@ZnO showed an excellent inhibition effect to *Aspergillus niger* and no black spores of *Aspergillus niger* existed onto other region of the plate (Fig. 5d). The results illustrated that the prepared wool-AO@ZnO achieves excellent anti-mould property. A similar result was reported by Hassan *et al.*[37] and Yu *et al.*[38]

After 24 h cultivation with *E. coli*, *S. aureus*, SRB, and *C. albicans*, the SEM profiles clearly showed that much more microorganisms were attached on the pristine wool fibers than on wool-AO@ZnO (Fig. 6). It suggests that the introduction of ZnO nanoparticles can impart the wool fibers with good antibacterial properties.

3.4. Antibacterial assessment by cyclic cultivation

The antibacterial properties of wool-AO@ZnO and its uranium(VI) adsorption were evaluated in 4 consecutive cyclic cultivations with bacteria. New living bacterial solutions were replaced after each measurement cycle. It can be seen that the inhibition rate of wool-AO@ZnO decreased after cultivation with *E. coli* and *S. aureus* (Fig. 7). After 4 cyclic cultivations, the inhibition rate decreased to 77.8% (*E. coli*) and 84.9% (*S. aureus*). The difference of their cell structure may cause the inhibition rate of *S. aureus* was higher than that of *E. coli*.[39] After four cyclic cultivations, uranium(VI) adsorption of wool-AO@ZnO still maintained at 46.5 mg g^{-1} (*E. coli*) and 57.6 mg g^{-1} (*S. aureus*). The results indicated that the wool-AO@ZnO has a good reusability property (Table 3).

4. Conclusions

To sum up, amidoxime-functionalized wool fibers loaded with nano-ZnO was successfully prepared by *in situ* coprecipitation and radiation-induced copolymerization. The introduction of

ZnO nanoparticles not only made the adsorbent an increase of uranium adsorption capacity but also imparted the adsorbent a good antimicrobial property. The adsorption process followed the Langmuir isotherm and psuedo-second-order kinetic. The maximum uranium adsorption capacity of wool-AO@ZnO was 96.2 mg g^{-1} from the Langmuir isotherm. Wool-AO@ZnO showed excellent antimicrobial properties to aerobic bacteria, anaerobic bacteria, and fungi. The inhibition of the bacteria *S. aureus* and *E. coli* growth could be up to 99.9%, and the inhibition of *C. albicans* could be at 92.6%. The inhibition of anaerobic bacteria SRB could be up to 95%. After 4 cycles' cultivation, the inhibition rate of *E. coli* and *S. aureus* can still keep the initial inhibition rate at 77.8% and 84.9%, while still maintained good adsorption capacity for uranium(VI). Therefore, the prepared wool-AO@ZnO showed a good prospect for extraction of uranium(VI) from seawater where multiple species of microorganisms exist.

Conflicts of interest

There are no conflicts to declare.

Acknowledgements

The authors gratefully thank to the financial support of the National Key Technology R&D Program of China (No. 2017YFB0308400) and the Opening Project of Key Laboratory of Leather Chemistry and Engineering, (Sichuan University), Ministry of Education, China (No. 20826041C4159).

References

1 V. Jegatheesan, B. K. Pramanik, J. Chen, D. Navaratna, C. Y. Chang and L. Shu, *Bioresour. Technol.*, 2016, **204**, 202–212.
2 P. G. Barbano and L. Rigali, *Anal. Chim. Acta*, 1978, **96**, 199–201.
3 J. C. B. S. Amaral and C. A. Morais, *Miner. Eng.*, 2010, **23**, 498–503.
4 T. V. Molchanova, L. I. Vodolazov, V. A. Peganov and V. G. Litvinenko, *At. Energy*, 2001, **90**, 208–212.
5 Q. Li, Y. Liu, X. Cao, C. Pang, Y. Wang, Z. Zhang, Y. Liu and M. Hua, *J. Radioanal. Nucl. Chem.*, 2012, **293**, 67–73.
6 Y. A. El-Nadi and J. A. Daoud, *J. Nucl. Radiochem. Sci.*, 2004, **5**, 11–15.
7 P. A. Brown, S. A. Gill and S. J. Allen, *Water Res.*, 2000, **34**, 3907–3916.
8 B. F. Parker, Z. Zhang, L. Rao and J. Arnold, *Dalton Trans.*, 2018, **47**, 639–644.
9 J. Qian, S. Zhang, Y. Zhou, P. Dong and D. Hua, *RSC Adv.*, 2015, **5**, 4153–4161.
10 Z. Yin, J. Xiong, M. Chen, S. Hu and H. Cheng, *J. Radioanal. Nucl. Chem.*, 2016, **307**, 1471–1479.
11 F. Zhang, M. Chen, S. Hu and H. Cheng, *J. Radioanal. Nucl. Chem.*, 2017, **314**, 1927–1937.
12 J. Wen, Q. Li, H. Li, M. Chen, S. Hu and H. Cheng, *Ind. Eng. Chem. Res.*, 2018, **57**, 1826–1833.
13 M. Monier, N. Nawar and D. A. Abdel-Latif, *J. Hazard. Mater.*, 2010, **184**, 118–125.
14 J. Park, G. A. Gill, J. E. Strivens, L. J. Kuo, R. T. Jeters, A. Avila, J. R. Wood, N. J. Schlafer, C. J. Janke and E. A. Miller, *Ind. Eng. Chem. Res.*, 2016, **55**, 4328–4338.
15 J. Hu, H. Ma, Z. Xing, X. Liu, L. Xu, R. Li, C. Lin, M. Wang, J. Li and G. Wu, *Ind. Eng. Chem. Res.*, 2015, **55**, 4118–4124.
16 H. Zhang, L. Zhang, X. Han, L. Kuang and D. Hua, *Ind. Eng. Chem. Res.*, 2018, **57**, 1662–1670.
17 M. Ranjbar-Mohammadi, M. Arami, H. Bahrami, F. Mazaheri and N. M. Mahmoodi, *Colloids Surf., B*, 2010, **76**, 397–403.
18 P. Zhu and G. Sun, *J. Appl. Polym. Sci.*, 2010, **93**, 1037–1041.
19 J. L. Castro-Mayorga, M. J. Fabra, A. M. Pourrahimi, R. T. Olsson and J. M. Lagaron, *Food Bioprod. Process.*, 2017, **101**, 32–44.
20 M. Wang, M. Zhang, L. Pang, C. Yang, Y. Zhang, J. Hu and G. Wu, *J. Colloid Interface Sci.*, 2019, **537**, 91–100.
21 H. Rodriguez-Tobias, G. Morales and D. Grande, *Mater. Chem. Phys.*, 2016, **182**, 324–331.
22 C. C. Okoro, *Liq. Fuels Technol.*, 2015, **33**, 1366–1372.
23 E. Guibal, C. Roulph and P. L. Cloirec, *Water Res.*, 1992, **26**, 1139–1145.
24 Z. Niu, Q. Fan, W. Wang, J. Xu, L. Chen and W. Wu, *Appl. Radiat. Isot.*, 2009, **67**, 1582–1590.
25 W. P. Li, X. Y. Han, X. Y. Wang, Y. Q. Wang, W. X. Wang, H. Xu, T. S. Tan, W. S. Wu and H. X. Zhang, *Chem. Eng. J.*, 2015, **279**, 735–746.
26 A. Degen and M. Kosec, *J. Eur. Ceram. Soc.*, 2000, **20**, 667–673.
27 H. R. Shakur, K. R. E. Saraee, M. R. Abdi and G. Azimi, *J. Mater. Sci.*, 2016, **51**, 1–14.
28 Ü. H. Kaynar, M. Ayvacıklı, S. Ç. Kaynar and Ü. Hiçsönmez, *J. Radioanal. Nucl. Chem.*, 2014, **299**, 1469–1477.
29 M. Khajeh and E. Jahanbin, *Chemom. Intell. Lab. Syst.*, 2014, **135**, 70–75.
30 W. Li, L. D. Troyer, S. S. Lee, J. Wu, C. Kim, B. J. Lafferty, J. G. Catalano and J. D. Fortner, *ACS Appl. Mater. Interfaces*, 2017, **9**, 13163–13172.
31 M. Solgy, M. Taghizadeh and D. Ghoddocynejad, *Ann. Nucl. Energy*, 2015, **75**, 132–138.
32 I. Langmuir, *J. Am. Chem. Soc.*, 1918, **40**, 1361–1403.
33 H. Freundlich, *J. Phys. Chem.*, 1906, **57**, 1100–1107.
34 R. Brayner, R. Ferrari-Iliou, N. Brivois, S. Djediat, M. F. Benedetti and F. Fiévet, *Nano Lett.*, 2006, **6**, 866–870.
35 A. Sirelkhatim, *Nano-Micro Lett.*, 2015, **7**, 219–242.
36 Y. Wang, Q. Zhang, C. L. Zhang and L. Ping, *Food Chem.*, 2012, **132**, 419–427.
37 M. M. Hassan, *ChemistrySelect*, 2017, **2**, 504–512.
38 D. Yu, W. Tian, B. Sun, Y. Li and W. Tian, *Mater. Lett.*, 2015, **151**, 1–4.
39 E. V. Skorb, L. I. Antonouskaya, N. A. Belyasova, D. G. Shchukin, H. Möhwald and D. V. Sviridov, *Appl. Catal., B*, 2008, **84**, 94–99.